

## Brief Reports

---

*Brief Reports are short papers which report on completed research which, while meeting the usual Physical Review standards of scientific quality, does not warrant a regular article. (Addenda to papers previously published in the Physical Review by the same authors are included in Brief Reports.) A Brief Report may be no longer than  $3\frac{1}{2}$  printed pages and must be accompanied by an abstract. The same publication schedule as for regular articles is followed, and page proofs are sent to authors.*

---

### Band folding and energy-gap formation in Ag-Au superlattices

T. Miller, M.A. Mueller, and T.-C. Chiang

*Department of Physics, University of Illinois at Urbana-Champaign, 1110 West Green Street, Urbana, Illinois 61801  
and Materials Research Laboratory, University of Illinois at Urbana-Champaign, 104 South Goodwin Avenue,  
Urbana, Illinois 61801*

(Received 6 February 1989)

The electronic band structures of superlattices consisting of alternating (111) slabs of Ag and Au were investigated with use of angle-resolved photoemission. The fundamental electronic effects of a superlattice potential, including band folding and the formation of energy gaps at the new zone boundaries, were clearly observed.

Through modern molecular-beam-epitaxy methods, a large variety of well-ordered crystalline heterostructures can be produced. The precise tailoring of these structures on an atomic scale gives the solid-state experimentalist vast opportunities to study interesting quantum-electronic effects and phenomena and to deduce important parameters for a fundamental understanding of the material properties. Much of the work in superlattice research has been carried out in semiconductor systems such as the GaAs/AlAs family, in which details of the electronic structure close to the band edges are accessible via methods like photoluminescence spectroscopy at low temperatures.<sup>1</sup> In comparison, there is little parallel research on the electronic properties of metallic superlattices for which most of the techniques developed for semiconductor systems are not applicable. Recent research on metallic superlattices has mainly focused on x-ray- and neutron-scattering studies of the structure and magnetic properties.<sup>2</sup>

In this work we explore the fundamental electronic effects of a superlattice modulation of the crystal potential by direct determination of the band structure using angle-resolved photoemission. The material chosen for this study, the Ag/Au superlattice, is particularly simple and can be considered a model system. The band structures of Ag and Au are very similar; within an energy window of about 2 eV below the Fermi level, only one nearly-free-electron-like *sp* band needs to be considered. We believe that this is the first time that band folding and the associated formation of gaps at the subzone boundaries are observed directly by photoemission, even though this technique has long been established as a

powerful (and perhaps unique) tool for mapping the valence-band dispersions. One difficulty involved in applying photoemission for band mapping is the relatively short probing depth, typically in the range 5–30 Å, which results in a significant momentum uncertainty; therefore, the superlattice period for this study is limited to rather small values for the effects to be clearly observable (a large period in real space corresponds to a small Brillouin zone). The lattice-matched Ag/Au system is one of the few metallic systems from which layer structures of small periods can be made with a high degree of perfection.

The photoemission experiments were performed using synchrotron radiation from the Aladdin storage ring at the Synchrotron Radiation Center (Stoughton, WI) of the University of Wisconsin–Madison. A 6-m toroidal-grating monochromator and a Seya monochromator were used in several different runs. Photoelectrons emitted along the sample–surface-normal direction were collected using a hemispherical electron-energy analyzer. The overall energy resolution was better than 0.2 eV. The starting substrate was a single-crystal Ag(111) prepared by mechanical polishing with 0.3- $\mu\text{m}$  alumina powder on a cloth pad lubricated with water, followed by electropolishing in a silver cyanide and potassium carbonate solution to remove a layer about 3  $\mu\text{m}$  thick from the surface.<sup>3</sup> It was repeatedly sputtered and annealed to generate a well-ordered and clean surface as verified by Auger spectroscopy, electron diffraction, and photoemission (observation of a sharp surface-state peak). A thick buffer layer of Ag was then grown on the substrate to further smooth out the surface; the improvement in smooth-

ness was evidenced by a decreased background in the high-energy electron-diffraction pattern. The superlattices were prepared by evaporation of Ag and Au from feedback-controlled electron-beam-heated tungsten crucibles. The rate of evaporation was monitored by a quartz thickness monitor. Based on calibration checks before and after deposition of each of the superlattices, the individual layer thicknesses should be consistent to within 1–2%. An absolute thickness calibration was also performed with an accuracy better than 10%.<sup>4</sup> The superlattice depositions were carried out with the sample at 30–50°C; this method has been shown to produce abrupt interfaces and good epitaxy.<sup>5,6</sup> All of the results reported here are for Ag-terminated superlattices with a total thickness of  $\sim 300$  Å. The Au-terminated superlattices show very strong Au  $5d$ -band emission in the spectral region of interest, causing severe interference with the measurement.

The photoemission spectra and the band structures for pure Au(111) and Ag(111) are very similar and have been discussed previously by various authors.<sup>7–14</sup> To facilitate the discussion we will regard the superlattice potential as a perturbation. Indeed, the photoemission spectra for the superlattices show an overall resemblance to those for either pure Au or Ag. Figure 1 shows representative normal-emission spectra from a sample consisting of alternating (111) slabs of Au and Ag of an equal thickness of 4 monolayers (ML; 1 ML = 2.36 Å). The range of pho-

ton energies used is the usual range used for mapping the uppermost  $sp$  valence band in Ag(111) and Au(111). The electron-escape depth is about 30 Å as determined from a separate measurement of the attenuation of the Ag (Au)-substrate  $d$ -band signal as a function of Au (Ag)-overlayer thickness. Each of the spectra has been normalized to the peak intensity of the (111) surface state; this is the large peak near the Fermi level which, for clarity, is shown only for the 9.0-eV scan. Both the Ag(111) and Au(111) surfaces support a surface state like the one shown in Fig. 1 for the superlattice; the binding energies are, however, slightly different.<sup>13–15</sup> On the high-binding-energy side of the bottom four spectra a large peak (labeled  $N$ , for normal process) can be seen which is due to direct transitions from the  $sp$  band. The dispersive behavior of this peak is similar to that observed in photoemission spectra of pure Ag(111) and Au(111) taken under identical conditions, except that the peak positions are somewhat different. This peak disperses toward higher binding energies with increasing photon energy and starts to overlap peaks from the Au  $d$  bands. The most important spectral features in Fig. 1, however, are the two smaller peaks (labeled  $U$ , for umklapp) which have no counterparts in the corresponding Ag(111) and Au(111) spectra. Evidently these  $U$  peaks are induced by the superlattice configuration. In the 10.0-, 10.5-, and 10.7-eV spectra, both peaks are simultaneously present, and it appears that there is a region around 1.3-eV binding energy that these peaks "avoid" as they shift as a function of photon energy. This is highly suggestive of photoemission mapping through a band gap.

To determine the valence-band dispersion relations, we need to know the final-band dispersion. For Ag(111) and Au(111) there is only one relevant final band in the range of photon energy used; thus, we expect the same for the superlattice system. Examination of several theoretical and experimental studies shows that the final bands in Ag and Au are very close within the region of interest.<sup>7–12,14</sup> In fact, the differences are generally less than the discrepancies between different determinations of the band for the same element. Since the differences are small, the final band for the superlattice system should resemble those of Ag and Au. The periodicity of the superlattice can cause formation of gaps in the final band. However, the size of the gap is expected to be no larger than about 0.5 eV (see below); therefore, the gaps in the final band can be ignored to the first order as the lifetime broadening and the presence of evanescent states within the gaps will tend to wash out any observable effects. Over the limited range of  $k$  values covered in these measurements, the final band of interest for either Ag or Au can be accurately approximated by a straight line. Therefore, we have adopted the following linear equation to describe the relevant portion of the final band in the superlattice:  $E = 15.2k/k_{\Gamma L} - 11.0$  eV, where  $E$  is in eV (relative to the Fermi level) and  $k_{\Gamma L}$  is the distance between the  $\Gamma$  and  $L$  points in the Brillouin zone for Ag and Au. This particular choice falls within the uncertainty range of the many published Ag and Au final bands.

Having defined the final state, we determine the valence-band structure using spectra like those shown in

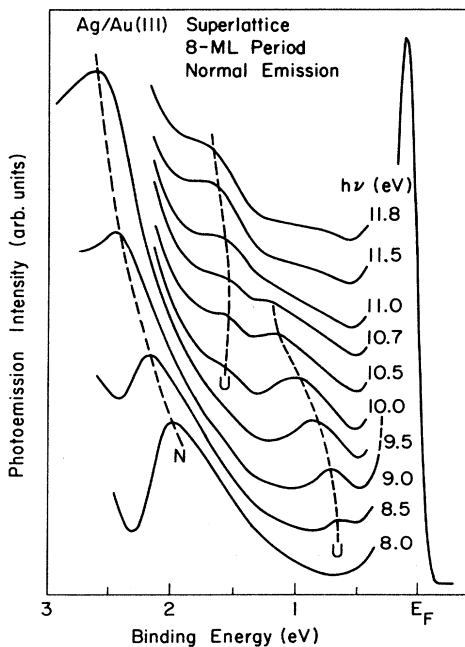


FIG. 1. Representative normal-emission photoemission spectra for a Ag/Au(111) superlattice with an 8-ML period. The photon energies ( $h\nu$ ) are indicated. Binding energies are referred to the Fermi level  $E_F$ . All of the spectra have been normalized to the peak height of the surface state (large peak shown partially only for the 9.0-eV spectrum), and have been displaced vertically for clarity. The dashed lines are a guide to the eye showing the movement of the three peaks as labeled.

Fig. 1.<sup>16</sup> Figure 2(a) shows the results for the sample discussed above. The solid squares correspond to the  $N$  peaks, while the solid circles correspond to the  $U$  peaks. The data are presented in the original Ag (Au) Brillouin zone from the  $\Gamma$  to the  $L$  point, since the superlattice potential is considered a perturbation here. The vertical dashed lines in Fig. 2 represent the new "Bragg planes" introduced by the superlattice periodicity, where superlattice gaps are expected to form after the unperturbed band is folded by the new periodicity. The spacing between neighboring Bragg planes equals one-half of the primitive reciprocal-superlattice vector. The open circles in Fig. 2(a) are obtained by translating the solid circles (derived from the  $U$  peaks) by a primitive reciprocal-superlattice vector to the right. The data from the  $U$  and  $N$  peaks are now joined smoothly together as they should be for truly superlattice-derived states.

Also shown in Fig. 2(a) are the Ag and Au  $sp$ -band dispersion curves. Due to the vacuum-level cutoff, the curves near the  $L$  point are not normally accessible by photoemission and have not been mapped. The curves shown are the combined results of several theoretical and experimental studies, and are somewhat uncertain ( $\Delta E \approx 0.1$  eV and  $\Delta k \approx 0.03 \text{ \AA}^{-1}$ ).<sup>5,7-15,17</sup> The Ag and Au dispersion curves and the corresponding "unfolded"

superlattice dispersion curves [solid squares and open circles in Fig. 2(a)] correlate very well. It is apparent that the result can be simply interpreted in terms of the superlattice potential as a perturbation which causes a gap to open up at the new zone boundary at  $k/k_{\Gamma L} = \frac{7}{8}$ . Note that the data from the solid squares in Fig. 2(a) (peaks from the normal process) are terminated just before reaching the superlattice gap at  $k/k_{\Gamma L} = \frac{7}{8}$ . This limit is due to the vacuum-level cutoff mentioned above. Note also that the  $U$  peaks are much weaker than the  $N$  peaks in the photoemission spectra, justifying our treatment of the superlattice potential as a perturbation.

Figure 2(b) shows a set of data taken from a superlattice with a period of 12 ML, again consisting of alternating slabs of Ag and Au of equal thickness. The same final band was used in the analysis. The results are very similar to those shown in Fig. 2(a). The solid squares and the open circles (obtained by translating the solid circles by a reciprocal-superlattice vector) are again joined together nicely. The gap now opens at a different location in the  $E$ -versus- $k$  diagram, in agreement with our model. This is strong evidence that our interpretation is correct. Note that there is no gap at  $k = \frac{10}{12}k_{\Gamma L}$ . This is not surprising because the superlattice modulation potential for equal Ag- and Au-slab thickness contains no even harmonics from a simple Fourier analysis; hence no gap is expected at this  $k$  value.

The uppermost miniband in these superlattices shows a dispersion intermediate between the corresponding Ag and Au dispersions, and lies above the Au band maximum. Within the energy range of this miniband, only nonpropagating (decaying) waves are allowed in bulk Au. Thus, if the interaction through the intervening Au slabs were zero, only states confined within individual Ag slabs (quantum-well states) could be observed, and there would be no band dispersion for this energy range.<sup>5</sup> Yet the miniband does show a significant dispersion, so the states observed here are not simple quantum-well states. This result provides a definitive proof of the interaction between neighboring Ag slabs and the presence of superlattice effects in this system. In each case presented in Fig. 2, the top portion of the dispersion curve for the lower unfolded miniband shows a relatively flat dispersion extending beyond the rightmost superlattice Bragg plane; the corresponding photoemission intensity diminishes for increasing  $k$ . The behavior just described can be attributed to residual emission from the band edge (critical point) of the lower miniband. The intensity variation of the peaks is indicative of band mapping across a Brillouin-zone boundary,<sup>18</sup> which provides further support for our present interpretation of the superlattice effects. Another point relevant to the present discussion concerns the coherence length of the electron wave function, which must be large compared with the superlattice period; indeed, this is supported by previous studies.<sup>5</sup>

We now comment on the size of the gap, which is about 0.3–0.4 eV for the data shown in Fig. 2. Within a nearly-free-electron approximation and a two-band model, the gap is twice the Fourier coefficient of the superlattice potential.<sup>19</sup> The average electrostatic potential difference between Ag and Au in contact can be estimat-

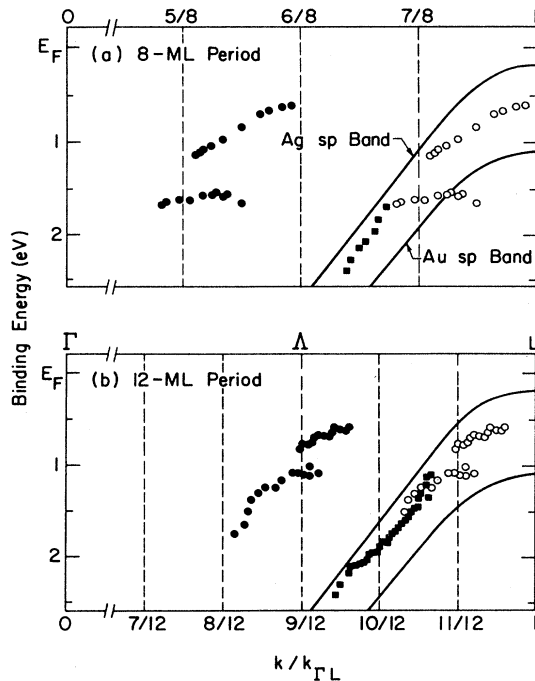


FIG. 2. Measured partial band structures for two superlattices with periods of (a) 8 ML and (b) 12 ML. The wave vector  $k$  is measured in terms of  $k_{\Gamma L}$ . The solid symbols are determined from peak positions in the photoemission spectra as described in the text. The open circles are obtained from the solid ones via a translation by a reciprocal-superlattice vector. Two of the open circles (the lowest two) in the lower panel are covered by the squares. The vertical dashed lines show the location of the Bragg planes of the superlattice. The band dispersions of the Ag and Au  $sp$  bands are also shown.

ed from previous thin-film studies, and is on the order of 0.1–0.3 eV.<sup>20</sup> Therefore, the size of the measured gap is consistent with this crude estimate. However, any attempt to apply the simple two-band model beyond this crude estimate is not warranted, since the measured gaps are not small compared with the energy widths of the minibands.

In summary, we have observed the basic electronic characteristics of superlattices, including the folding of the bands and the formation of energy gaps. This study illustrates the general process of band-structure formation in periodic systems under direct experimental control. The very many possibilities of creating different material structures and observing new and interesting electronic effects make this demonstration of fundamental importance. Specifically, the present results including the band dispersions and gaps should provide valuable input to a theoretical understanding and the modeling of the Ag/Au interface properties and modulation effects.

#### ACKNOWLEDGMENTS

This material is based on work supported by the U. S. National Science Foundation (NSF) under Contract No. DMR-86-14234. Some of the personnel and equipment were also supported by grants from the NSF (Grant No. DMR-83-52083), the IBM Thomas J. Watson Research Center (Yorktown Heights, NY), and the E. I. duPont de Nemours and Company (Wilmington, DE). The Synchrotron Radiation Center (Stoughton, WI) of the University of Wisconsin–Madison is supported by the NSF under Contract No. DMR-80-20164. We acknowledge the use of central facilities of the Material Research Laboratory of the University of Illinois, which is supported by the U. S. Department of Energy (Division of Materials Sciences of the Office of Basic Energy Sciences), under Contract No. DE-AC02-76ER01198, and the NSF under Contract No. DMR-86-12860.

<sup>1</sup>See, for example, E. E. Mendez, F. Agulló-Rueda, and J. M. Hong, *Phys. Rev. Lett.* **60**, 2426 (1988).

<sup>2</sup>See, for example, the articles in *Metallic Multilayers and Epitaxy*, edited by M. Hong, D. U. Gubser, and S. A. Wolf (The Metallurgical Society, Warrendale, PA, 1988).

<sup>3</sup>W. J. McG. Tegart, *The Electrolytic and Chemical Polishing of Metals* (Pergamon, London, 1956).

<sup>4</sup>Based on a variation of the method reported by A. P. Shapiro, A. L. Wachs, and T.-C. Chiang, *Solid State Commun.* **58**, 121 (1986).

<sup>5</sup>T. Miller, A. Samsavar, G. E. Franklin, and T.-C. Chiang, *Phys. Rev. Lett.* **61**, 1404 (1988).

<sup>6</sup>R. J. Culbertson, L. C. Feldman, P. J. Silverman, and H. Boehm, *Phys. Rev. Lett.* **47**, 657 (1981).

<sup>7</sup>J. G. Nelson *et al.*, *Phys. Rev. B* **32**, 3465 (1985); S. Wehner *et al.*, *ibid.* **19**, 6164 (1979).

<sup>8</sup>K. A. Mills *et al.*, *Phys. Rev. B* **22**, 581 (1980); R. Courths *et al.*, *Solid State Commun.* **49**, 989 (1984).

<sup>9</sup>R. Courths, H. G. Zimmer, A. Goldmann, and H. Saalfeld, *Phys. Rev. B* **34**, 3577 (1986).

<sup>10</sup>H. Eckardt, L. Fritsche, and J. Noffke, *J. Phys. F* **14**, 97 (1984).

<sup>11</sup>N. E. Christensen, *Phys. Status Solidi B* **54**, 551 (1972).

<sup>12</sup>N. E. Christensen and B. O. Seraphin, *Phys. Rev. B* **4**, 3321 (1971).

<sup>13</sup>T. C. Hsieh, T. Miller, and T. C. Chiang, *Phys. Rev. Lett.* **55**, 2483 (1985); R. C. Jaklevic and J. Lambe, *Phys. Rev. B* **12**, 4146 (1975); R. Rosei, C. H. Culp, and J. H. Weaver, *ibid.* **10**, 484 (1974); D. P. Woodruff, W. A. Royer, and N. V. Smith, *ibid.* **34**, 764 (1986); N. V. Smith, *ibid.* **32**, 3549 (1985); L. Wallden and T. Gustafsson, *Phys. Scr.* **6**, 73 (1972).

<sup>14</sup>S. H. Liu *et al.*, *J. Electroanal. Chem.* **176**, 325 (1984); K.-M. Ho *et al.*, *ibid.* **150**, 235 (1983).

<sup>15</sup>T. C. Hsieh and T.-C. Chiang, *Surf. Sci.* **166**, 554 (1986).

<sup>16</sup>See, for example, F. J. Himpsel, *Appl. Opt.* **19**, 3964 (1980).

<sup>17</sup>S. D. Kevan and R. H. Gaylord, *Phys. Rev. B* **36**, 5809 (1987).

<sup>18</sup>See, for example, R. Courths and S. Hüfner, *Phys. Rep.* **112**, 53 (1984).

<sup>19</sup>See, for example, N. W. Ashcroft and N. D. Mermin, *Solid State Physics* (Saunders College, Philadelphia, PA, 1976), pp. 151–162.

<sup>20</sup>T. C. Hsieh, T. Miller, and T.-C. Chiang, *Phys. Rev. B* **33**, 2865 (1986); T. C. Hsieh, A. P. Shapiro, and T.-C. Chiang, *ibid.* **31**, 2541 (1985).